Proceedings, 5th Int'l. Conf. on Plasma Surface Interactions in Controlled Fusion Devices, May 3-7, 1982, Gatlinburg, TN

Effect of Oxygen Monolayer Coverages on Titanium Sputtering Yields as Determined by Simultaneous Laser Fluorescence and Auger Measurements*

M. J. Pellin, C. E. Young, M. H. Mendelsohn, D. M. Gruen

R. B. Wright,+ and A. B. DeWald,++ Chemistry Division,

Argonne National Laboratory, Argonne, Illinois 60439

The presence of an oxide layer can strongly influence the charge-state of species ejected from ion-bombarded metal surfaces, as well as the total sputtering yield. These quantities directly affect the influx of metallic impurities from the wall region into the plasmas of fusion devices. Surface coverage can also modify the distribution of sputtered atoms among electronic states and thus the apparent impurity density detected by the laser fluorescence spectroscopy (LFS) technique. The measurements reported here provide LFS data on number density and electronic state populations for the species Ti and Ti^+ as a function of surface oxygen coverage in a laboratory apparatus providing for direct monitoring by Auger analysis. An ultra-high vacuum chamber reached a base pressure of $\leq 10^{-8}$ Pa after 200°C bakeout, making target contamination negligible during data collection. A target holder with translation and rotary motions, positioned in the center of the chamber, could be turned to face the Auger analysis station or a 3 keV sputter ion gun (180° apart in the horizontal plane). A second identical ion gun was aimed down at 20° to the laser beam, which was directed vertically. A Nd:YAG pumped pulsed dye laser (10 Hz, 15 ns pulse) was used for

*Work performed under the auspices of the Office of Basic Energy Sciences, Division of Materials Sciences, U. S. Department of Energy under Contract 31-109-ENG-38.

+Present Address: UOP., Corporate Research Center, 10 UOP Plaza, Des Plaines, IL 60016

++A. B. DeWald, Dept. of Nuclear Engineering, Georgia Institute of Technology, Atlanta, GA 30332

excitation with a bandwidth of $\sim$1 cm^{-1} for total fluorescence yield measurements. Ion bombardment was either continuous (typically 20 μA of Ar^+ on a 3 mm dia. region) or in a low erosion mode providing a short interval of sputtering in synchronism with each laser pulse. The target could be dosed with oxygen via a directed stream or through controlled leakage into the chamber. Data to be presented span the regime between a clean metal surface and three monolayer coverage.

1. Introduction

Oxide coatings are inevitably present on the walls of plasma-confinement devices, at least in the initial stages of each discharge. The presence of oxygen has been observed to produce a lowering of the sputtering yield of metal atoms in experiments using the weight-loss technique [1] and by SIMS analysis of the sputtering of thin films [2]. In the case of titanium, oxygen has also been shown to produce a strong increase in the secondary ion yield [2-4]. The conclusion that a considerable fraction of the metal sputtered from a suitably oxidized surface is in the ionized state has led to the suggestion that this condition be exploited to impede the flow of impurity atoms into plasma discharges in fusion devices [5].

The effect of oxygen on the sputtering yield of iron [6] and titanium [7] has recently been studied by the method of laser-induced fluorescence (LFS). As in some of the earlier oxidation work, dynamic balance was maintained between erosion of the metal surface by sputtering and oxide formation due to a static pressure of O_2. This produces an oxide coating characteristic of the bombardment conditions, which can be very different from that obtainable by prior deposition of surface films [8].

The present work represents an attempt to gain more information about the nature of the oxidized metal surface by direct monitoring by Auger electron spectroscopy, while measuring sputtering yields by the LFS technique. The kinetics of the AES oxygen signal decay, as sputtering proceeded was used to obtain the sputtering yield for that component directly. Changes in the erosion rate were observed at reproducible Auger oxygen to titanium peak signal ratios, permitting inferences about surface conditions. For titanium the sputtering yield relative to that characteristic of the bare metal was obtained for initial oxygen coverages equivalent to 3 monolayers, for each state of the $a^3F_{2,3,4}$ ground multiplet. Similar data was obtained for the a^5F_5 excited state, along with less comprehensive coverage studies for several other low-lying excited states. A pulsed ion source, in synchronism with the pulsed laser employed was introduced to minimize the erosion rate of the oxide film.

2. Experimental

The experiments were conducted in the UHV chamber illustrated in Fig. 1. A main pumping system consisting of a 200 l/s ion pump plus titanium sublimator produced a 10^{-8} Pa base pressure after 200°C bakeout. This permitted typical 1h runs with negligible contamination of the titanium target. The targets were polycrystalline Ti disks of 1.4 cm diameter and 0.3 mm thickness, mounted on a translation/rotation stage. This arrangement allowed the target to be turned to face the AES unit (Physical Electronics, Model 10-234-G) and scanned in a direction perpendicular to the incident electron beam for examining surface contamination, and determining ion beam profiles eroded into an oxygen-treated surface. The ion beam was obtained from a commercial ion-source (Varian Associates, Model 981-2043) producing currents of 3 keV Ar^+ of 10-20 μA in a 3 mm dia. best focus spot. Operation of this source required back filling of the chamber with

the working gas (Ar); a pressure of 8×10^{-3} Pa was normally used.

The ion source was operated in pulsed mode by application of a brief flat topped pulse (4 μs duration), producing a 600 V potential difference across the deflection plate system of the ion gun. This produced a deflection of about 6 mm at the target, for 3 keV ions. The target was aligned so that the deflected beam reached the target center. During most of the time between laser pulses (100 ms) the undeflected beam impacted the edge of the Ti target region, which was kept free of protruberances above the flat surface to minimize the deposition of sputtered material on the central area. The off axis arrangement was necessary to keep a small component of charge exchanged fast neutrals from eroding the working region.

The dye laser system (Molectron MY34-DL16) was synchronized to fire at about 3 μs after the ion beam was pulsed to the center of the target. For the present experiments, broadband operation ($\sim$1 cm^{-1} linewidth) was employed, with sufficient power for high saturation of the pumped transitons. The beam passed through the vacuum chamber several mm in front of the deflected ion beam position. Detection optics focused this region into an 0.3 m grating monochromator. Various filters in the optical path reduced scattered laser light. Detection was via a cooled photomultiplier and pulse counting system. Details of the laser system and LFS techniques have been published [9,10].

An inlet to the vacuum chamber provided capability for directing a stream of oxygen onto the target during sputtering. In most cases this method was not employed, however, and the target was oxygen-coated in a position facing the AES system, after sputter-cleaning. The oxygen partial pressure ($\sim 10^{-6}$ Pa) was monitored with a quadrupole gas analyzer. In accordance with the high sticking coefficient, for oxygen on titanium [11], one monolayer coverage

was achieved at exposures of 1-2 L, while 5L was sufficient to produce an AES signal corresponding to about 3 monolayers. Desorption of oxygen by the AES electron beam could be easily observed above the second monolayer but could be kept to an acceptable rate by minimizing the beam current.

3. Results and discussion

3.1 Oxide sputtering kinetics

The erosion of the oxygen near-surface layer by a steady beam of ions of current density J ions/cm^2 can be described in terms of a cross section σ for the desorption process by

$$\sigma = \frac{d \ln y}{dt} / J = S/n_o \qquad (1)$$

where S atoms/ion is the sputtering yield at one monolayer coverage, n_o atoms/cm^2 the area density for one monolayer, and y is any quantity proportional to actual surface coverage n(t) atoms/cm^2. Here we take for y the AES O/Ti signal ratio from the peak heights of the 510 eV oxygen and the 418 eV titanium lines in the differential Auger spectrum. While the sputtering process is not strictly an describable by a cross section for independent ejection events, the approximation seems good for low coverage [12,13]. In Fig. 2 where the O/Ti Auger ratio is plotted against time (for a beam current density of 2×10^{14} ions $cm^{-2}s^{-1}$ at the monitoring position), four distinct regions of slope, labelled A-D can be identified. The assignment of oxygen coverage values, given in Table I is deduced from a simple model of the expected O/Ti Auger peak ratio as a function of coverage. As is discussed below, this is strongly supported by experimental evidence from other studies. Also given in Table I are the σ and S values calculated from Eq. 1 for a value of

$n_o = 1.474 \times 10^{15}$ atoms/cm^2. For n_o the 2/3 power of the Ti atom density in the hcp metal crystal was taken as an estimate appropriate to the polycrystalline sample in use.

In obtaining the data of Fig. 2, care was taken to roster the ion beam spot over an area at least twice the nominal beam FWHM diameter, while taking AES data as close to the peak of the time averaged erosion profile as possible. The profile was modelled with a Gaussian function to relate current density at the AES beam position to total target ion current. Secondary electrons were suppressed with a +90 V bias applied to the target.

A simple estimate of the O/Ti AES peak ratio expected for one monolayer of oxygen coverage on Ti metal comes from noting the (almost equal) atom sensitivities for the O 510 eV and Ti 418 eV lines involved [14] and summing over layers spaced by the average Ti atom-atom distance in the metal (s = 2.604 Å) and attenuated by the factor exp(-s/a) where a is taken to be 9 Å for either line, an approximation based on the universal escape depth function [15]. This formulation predicts an O/Ti ratio of 0.39 in the AES differential spectrum and is not very sensitive to the exact position of the O atoms in the near surface region. Evidence supporting this view comes from LEED data [16] where a characteristic p (2x2) pattern corresponding to 1/4 monolayer of oxygen is observed at an AES peak ratio of $\sim$0.1. This tightly bound layer would correspond to the D region of Fig. 2 having the lowest sputtering yield and with a transition from the C region also at O/Ti (AES) of $\sim$.1. In addition, a change in slope at this point has been seen in the kinetics of oxidation [17]. It should be noted that Taglauer and co-workers [18] have reported a transition to a region of much slower desorption, occurring after the erosion of about one monolayer, which would correspond to the C-D break in our Fig. 2.

3.2 LFS measurements of Ti sputtering yield.

Sputtering experiments with LFS detection were performed successively on each member of the a^3F_J, J = 2,3,4 ground state multiplet, with excitation and detection wavelengths selected from the $a^3F \rightarrow z^3F^o$ system at ∿520 nm. The energy levels [19] and radiative lifetimes [20] for this system are given in Fig. 3. A maximum of 6 nm separation between excitation and detection wavelengths was possible, requiring the use of interfere filters in series with the monochromator in order to attenuate stray laser light. To monitor the dependence of the sputtering yield on oxygen coverage, exposure to a few L of O_2 was performed, as described in Section 3.1. At the start of the LFS experiment, rapid erosion of the oxygen film imposed the requirement of short accumulation times (e.g. 10s). Sufficient Auger data was acquired to allow the assignment of an O/Ti ratio to each photon accumulation interval, by interpolation. The LFS signal was followed through diminishing oxygen coverage until essentially bare metal was indicated by the AES system, at the center of impact of the pulsed ion-beam position. The relative normalization of the curves for the different fine-structure states in Fig. 3 was obtained by separate experiments on the clean metal target for each of the J = 2,3 and 4 levels. Corrections for the differing degeneracies, radiative lifetimes and branching ratios at the detection wavelength were applied. The resulting ratios indicated in Fig. 4 imply a statistical population of the J = 2-4 levels at ∿300K. Furthermore, this situation is preserved up to the maximum oxygen coverage employed since when normalized to the same ordinate, all three curves in the figure have the same slope, within experimental uncertainty. To achieve absolute calibration of the data, the sum of the 3 ordinates at zero coverage was equated to the value of S for Ar^+ on Ti, calculated at 3 keV from published

experimental values at other energies [8,21], scaled via Sigmund theory [22], giving the value S ≈ 1.1. A further tacit assumption in interpreting the data of Fig. 4 as sputtering yields is that the velocity of the ejected Ti atoms does not vary substantially with oxygen coverage or the state of the ejected species. Large errors are not expected to arise from these effects, but velocity distribution data will be required to resolve the question.

LFS monitoring of atoms in states within a few eV of the ground state failed to discover any state growing to sufficient population to account for the loss of ground multiplet population at increasing oxygen coverage. This implies that the decrease observed in Fig. 4 must be attributed entirely to reduced numbers of atoms sputtered as oxygen coverage increases.

Different behavior was seen for atoms sputtered into the a^5F_5 level at 6843 cm^{-1}. As seen in Fig. 5, oxygen coverage enhances the observed occupation of this state, in the first excited multiplet of TiI. Since some reduction in the total sputtering yield of metal atoms is expected (and confirmed by Fig. 4), we conclude that the effect of surface oxygen is to enhance the excitation probability into a^5F_5 more than enough to compensate the loss over overall atoms sputtered. The effect seems even more pronounced for higher lying levels (Table II).

A search was also made for atoms sputtered into low levels of Ti^+ using transitions near 300 nm. No Ti^+ signal was identifiable when sputtering from targets coated as above with oxygen in the 0 to 3 monolayer regime. From this it was estimated that the population of ions in the state being probed is less than 1% of the neutral ground state Ti population, sputtered from these oxide surfaces. This conclusion, which was also reached by Dullni and Hintz [7] may be reconciled with the high Ti^+ fraction results seen by other techniques by assuming that the ion population is rather uniformly distributed over many spectroscopic states, in contrast with the situation for neutral Ti atoms.

3.3 Computer sputtering calculations.

The noteworthy features of the sputtering yields found in this work are (i) the weak dependence of titanium sputtering yield on oxygen coverage and (ii) the small yield for desorption of O atoms. In order to understand the physical basis for the results observed some model calculations were performed with the TRIM code of Haggmark and Biersack [23,24], modified to include multiple layers and components for sputtering calculations. Sample calculations are illustrated in Fig. 6, where the experimental values of the sputtering yield for titanium S(Ti) and for oxygen S(O) are also plotted for coverages of one and two monolayers. In the limit of zero coverage S(O) = 0 and S(Ti) = 1 on the plot. The lowest of the S(Ti) curves and the highest S(O) curve (narrow lines in Fig. 6) proceeding from zero toward higher O/Ti atom ratio, correspond to a model with O atoms depositing over the top Ti layer. The bulk heat of sublimation E_s for titanium metal, 4.9 eV [25] is retained for both the O and Ti species as the surface planar energy barrier criterion for sputtering in this case. Between 1 and 2 monolayers, a choice is permitted between putting the second oxygen above or below the topmost Ti layer, bracketing the shaded regions. It is found that increasing E_s will lower S(O) with a possibility of fair agreement with experiment at $E_s \simeq 10$ eV but no corresponding increase can be produced in the sputtering yield for Ti, which is shielded by the O atom overlayer. A second possibility is demonstrated by the medium-width lines namely deposition of the first oxygen monolayer under the Ti upper layer. This has been shown to be the actual morphology for N_2 on Ti [26], for example. This effectively lowers S(O) but S(Ti) is still too low. However, now the outer O-Ti bond can be made weaker without inducing significant change in S(O). The choice of E_s = 3 eV for Ti (keeping E_s = 4.9 for O) is illustrated in the heaviest curves of Fig. 6, producing good agreement with experiment at O/Ti = 1

monolayer. Since it was assumed that the second layer should go on top of the Ti in this case, the agreement deteriorates between 1 and 2 monolayers. It seems possible in the real case, however that some of the oxygen may go into the bulk between 1 and 2 monolayer coverage as seen by the AES. This could restore the agreement with experiment, with 1.5 monolayers, say, on the calculated curves being appropriate to an apparent 2 monolayers in the experiment.

A question remains as to whether the binding energy E_s for Ti with an oxygen underlayer could be as small as 3 eV, as assumed. However, the oxygen-underlayer model seems to do the best at explaining the data.

References

1. J. Hrbek, Thin Solid Films 42 (1977) 185.
2. W. O. Hofer and P. J. Martin, Appl. Phys. 16 (1978) 271.
3. A. Muller and A. Benninghoven, Surf. Sci. 41 (1974) 493.
4. A. R. Krauss and D. M. Gruen, Nucl. Instrum. Methods 149 (1978) 547.
5. A. R. Krauss and D. M. Gruen, J. Nucl. Mater. 63 (1976) 380.
6. R. Behrisch, J. Roth, J. Bohdansky, A. P. Martinelli, B. Schweer, D. Rusbült, and E. Hintz, J. Nucl. Mater. 93 & 94 (1980) 645.
7. E. Dullni and E. Hintz, private communication.
8. W. O. Hofer, H. L Bay, and P. T. Martin, J. Nucl. Mater. 76 & 77 (1978) 156.
9. R. B. Wright, M. J. Pellin and D. M. Gruen, Surf. Sci. 110 (1981) 151.
10. R. B. Wright, M. J. Pellin and D. M. Gruen, Nucl. Instrum. Methods 182 & 183 (1981) 167.
11. E. Fromm and O. Mayer, Surf. Sci. 74 (1978) 259.
12. E. Taglauer, G. Marin, W. Heiland and U. Beitat, Surf. Sci. 63 (1977) 507.
13. H. F. Winters and P. Sigmund, J. Appl. Phys. 45 (1974) 4760.

14. L. E. Daris, N. C. MacDonald, P. W. Palmberg, G. E. Riach, and R. E. Weber, Handbook of Auger Electron Spectroscopy, 2nd. edition (Physical Electronics Division, Perkin-Elmer Corp.)

15. A. Joshi, L. E. Davis and P. W. Palmberg in "Methods of Surface Analysis", A. W. Czanderna, Ed., Elservier, NY 1975, p. 164.

16. B. T. Jonker, J. F. Moran and R. L. Park, Phys. Rev. B 24 (1981) 2951.

17. H. D. Shih and F. Jona, Appl. Phys. 12 (1977) 311.

18. E. Taglauer, W. Heiland and R. J. MacDonald, Surf. Sci. 90 (1979) 661.

19. C. E. Moore, Atomic Energy Levels, NSRDS-NBS35 U. S. Government Printing Office, Vol. I.

20. W. L. Wiese and J. R. Fuhr, J. Phys. Chem. Ref. Data 4 (1975) 263.

21. N. Lagreid and G. K. Wehner, J. Appl. Phys. 32 (1961) 365.

22. P. Sigmund, Phys. Rev. A 184 (1969) 383.

23. J. P. Biersack and L. G. Haggmark, Nucl. Instrum. Methods 174 (1980) 257.

24. L. G. Haggmark and J. P. Biersack, J. Nucl. Mater. 93 & 94 (1980) 664.

25. JANAF Thermochemical Tables, NSRDS-NBS 37, U.S. Government Printing Office, 1971.

26. H. D. Shih and F. Jona, Surf. Sci. 60 (1976) 445.

Table 1. Sputtering yield data from erosion kinetics of O/Ti Auger signal.

region (Fig. 2)	O/Ti (Auger) at slope change	coverage (monolayers)	S (atoms/ion)	σ (10^{-16} cm^2)
A	A-B = 0.92	> 2	1.9	13
B	B-C = 0.39	1 - 2	0.35	2.4
C	C-D = 0.15	.25 - 1	0.20	1.4
D		0 - .25	0.11	0.7

Table 2. Enhancement of population of several low lying Ti^{o} states by ~2 monolayer oxygen coverage.

State	Energy (cm^{-1})	Signal (oxidized)/Signal (clean)
a^3F_2	0	0.38
a^3F_3	170	0.46
a^3F_4	387	0.63
a^1D	7255	4.3
a^5F_4	6743	3.3
b^3F_4	11777	4.7
z^3F^o	19574	4.9*

*excited state emission, not laser fluorescence.

Figure Captions

Fig. 1. The UHV laser-fluorescence apparatus. A quadrupole residual gas analyzer (not shown) monitors the chamber.

Fig. 2. The kinetics of oxygen removal as monitored by AES at a position on the target receiving a current density of 2×10^{14} ions/cm^2·sec (3 keV Ar^+). Four distinct erosion rates are identified A-D.

Fig. 3. Spectroscopic data on the line system used for LFS study of Ti sputtering from the lowest states.

Fig. 4. Ti LFS signal as a function of O/Ti AES signal for the lowest multiplet.

Fig. 5. Ti LFS signal as a function of O/Ti AES signal, for a member of the first excited Ti multiplet.

Fig. 6. Experimental results of this work compared with predictions of TRIM sputtering code, both experiment and theory normalized to S(Ti) = 1 at zero oxygen coverage. Solid curves: S(Ti), dashed curves S(O). Oxygen may be placed over or under the top layer of Ti atoms (see Legend and Section 3.3).

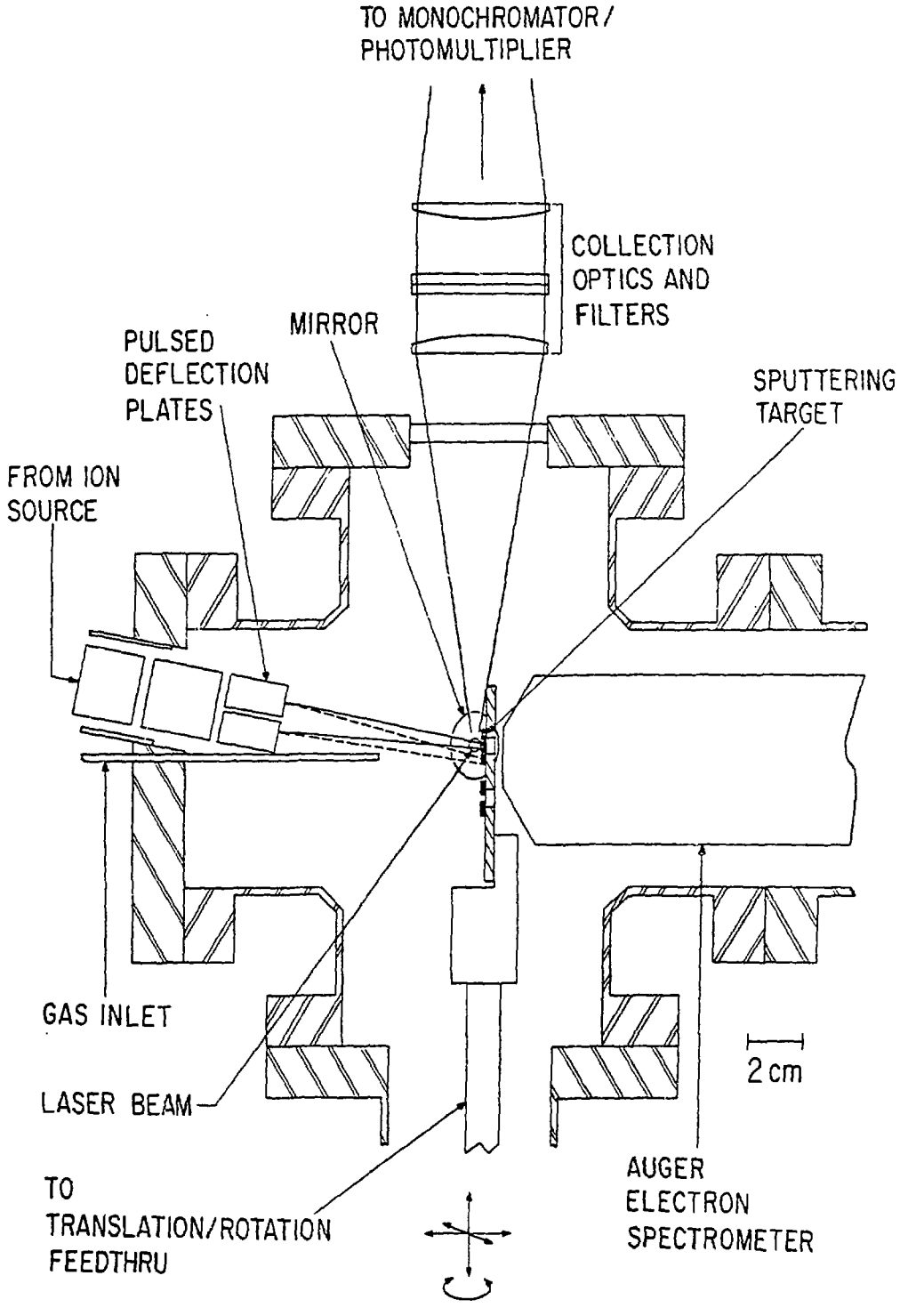
TO MONOCHROMATOR/
PHOTOMULTIPLIER
COLLECTION
OPTICS AND
FILTERS
MIRROR
PULSED
DEFLECTION
PLATES
SPUTTERING
TARGET
FROM ION
SOURCE
GAS INLET
LASER BEAM
TO
TRANSLATION/ROTATION
FEEDTHRU
AUGER
ELECTRON
SPECTROMETER
2 cm

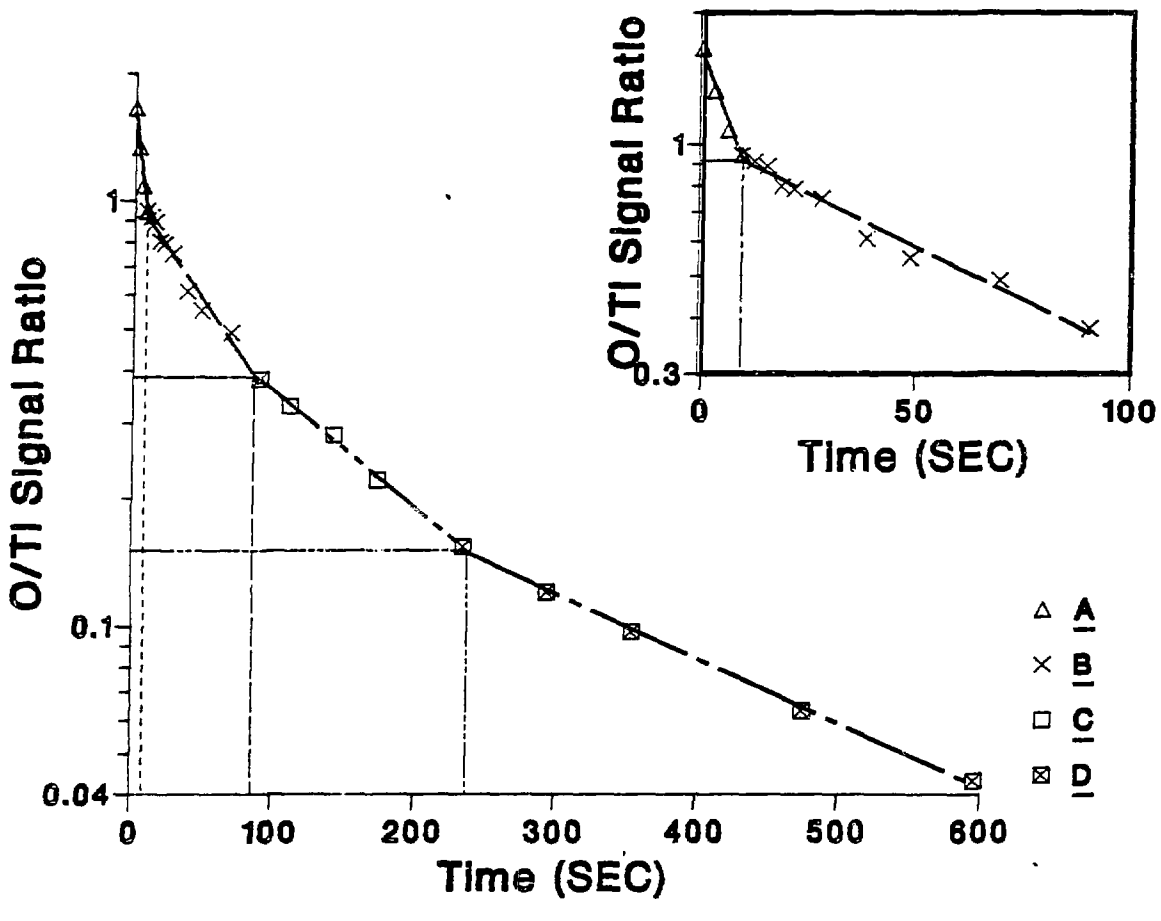
O/TI Signal Ratio
1
0.1
0.04
0
100
200
300
400
500
600
Time (SEC)
O/TI Signal Ratio
1
0.3
0
50
100
Time (SEC)
A
B
C
D

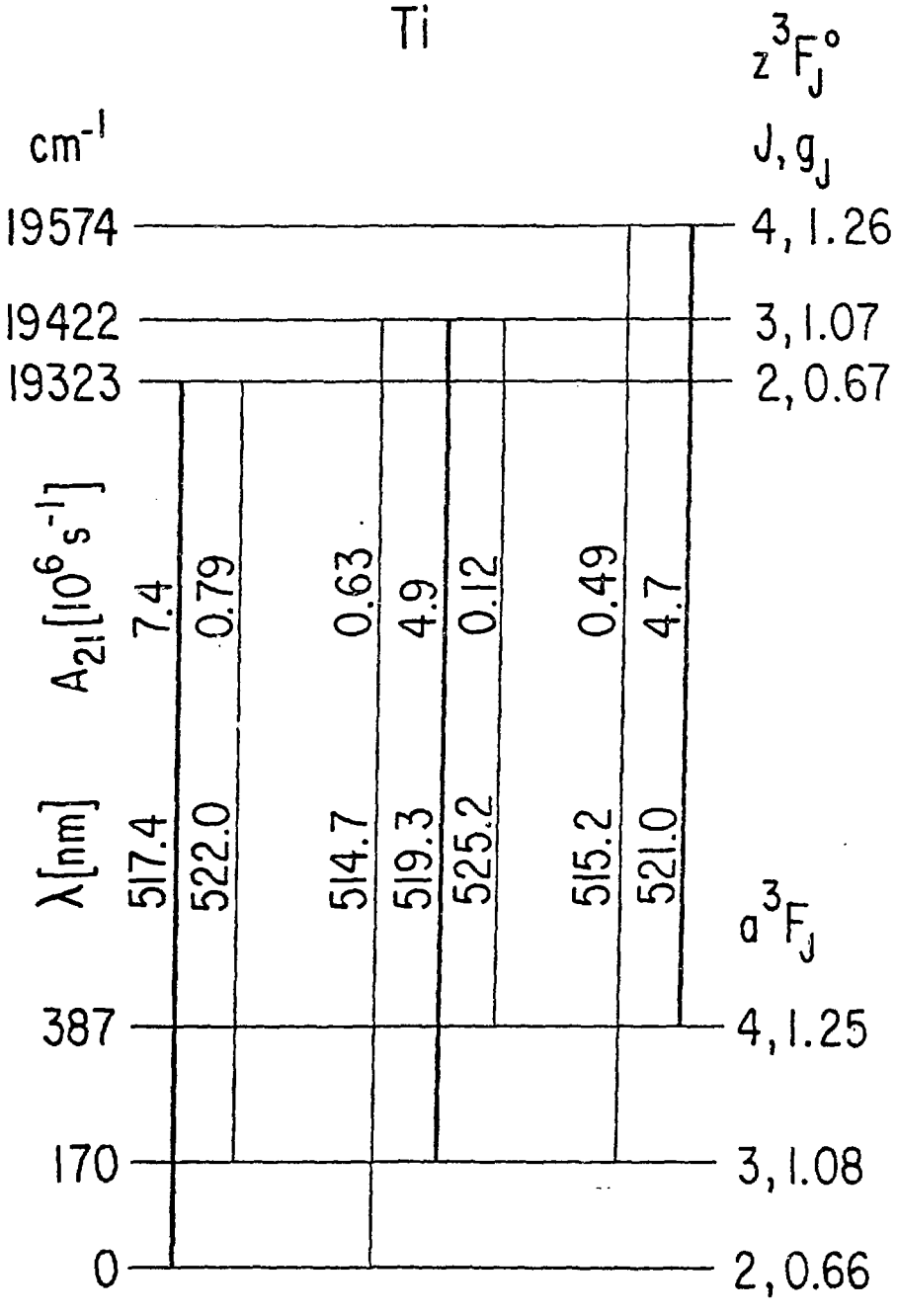
Ti
$z^3F_J^\circ$
cm^{-1}
J, g_J
19574
19422
19323
4, 1.26
3, 1.07
2, 0.67
$A_{21}[10^6 s^{-1}]$
λ[nm]
7.4
517.4
0.79
522.0
0.63
514.7
4.9
519.3
0.12
525.2
0.49
515.2
4.7
521.0
a^3F_J
387
170
0
4, 1.25
3, 1.08
2, 0.66

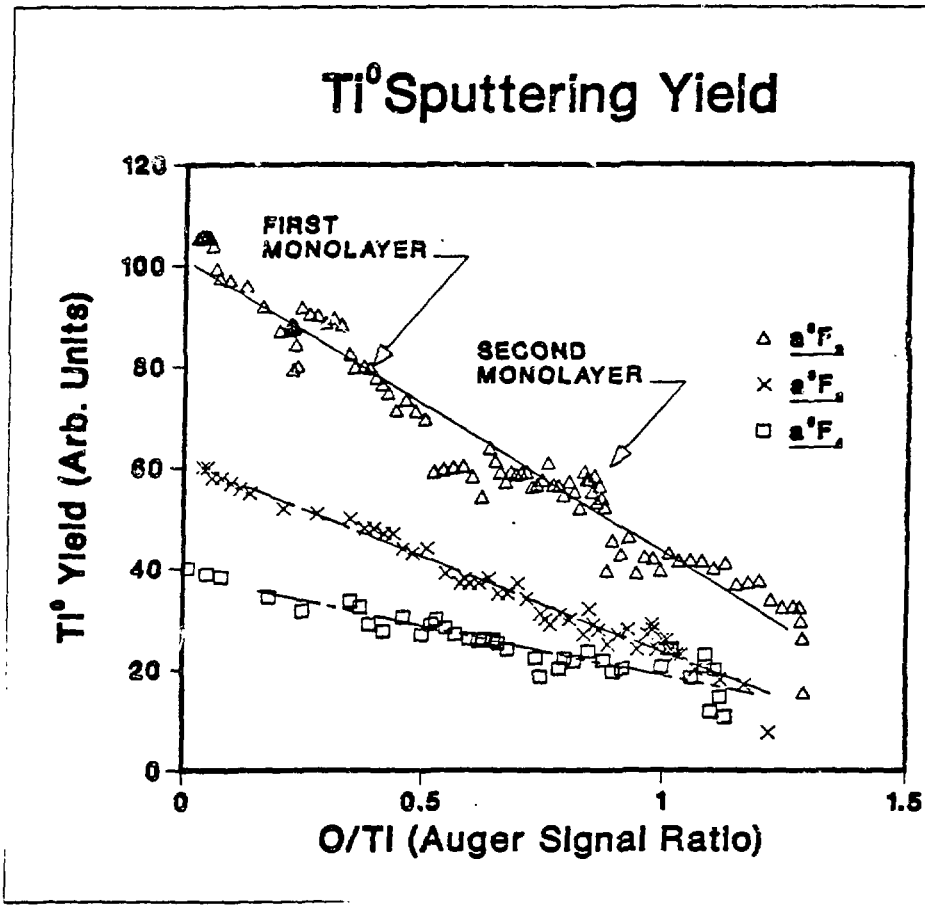
Ti⁰ Sputtering Yield
FIRST MONOLAYER
SECOND MONOLAYER
Ti⁰ Yield (Arb. Units)
O/Ti (Auger Signal Ratio)
120
100
80
60
40
20
0
0
0.5
1
1.5

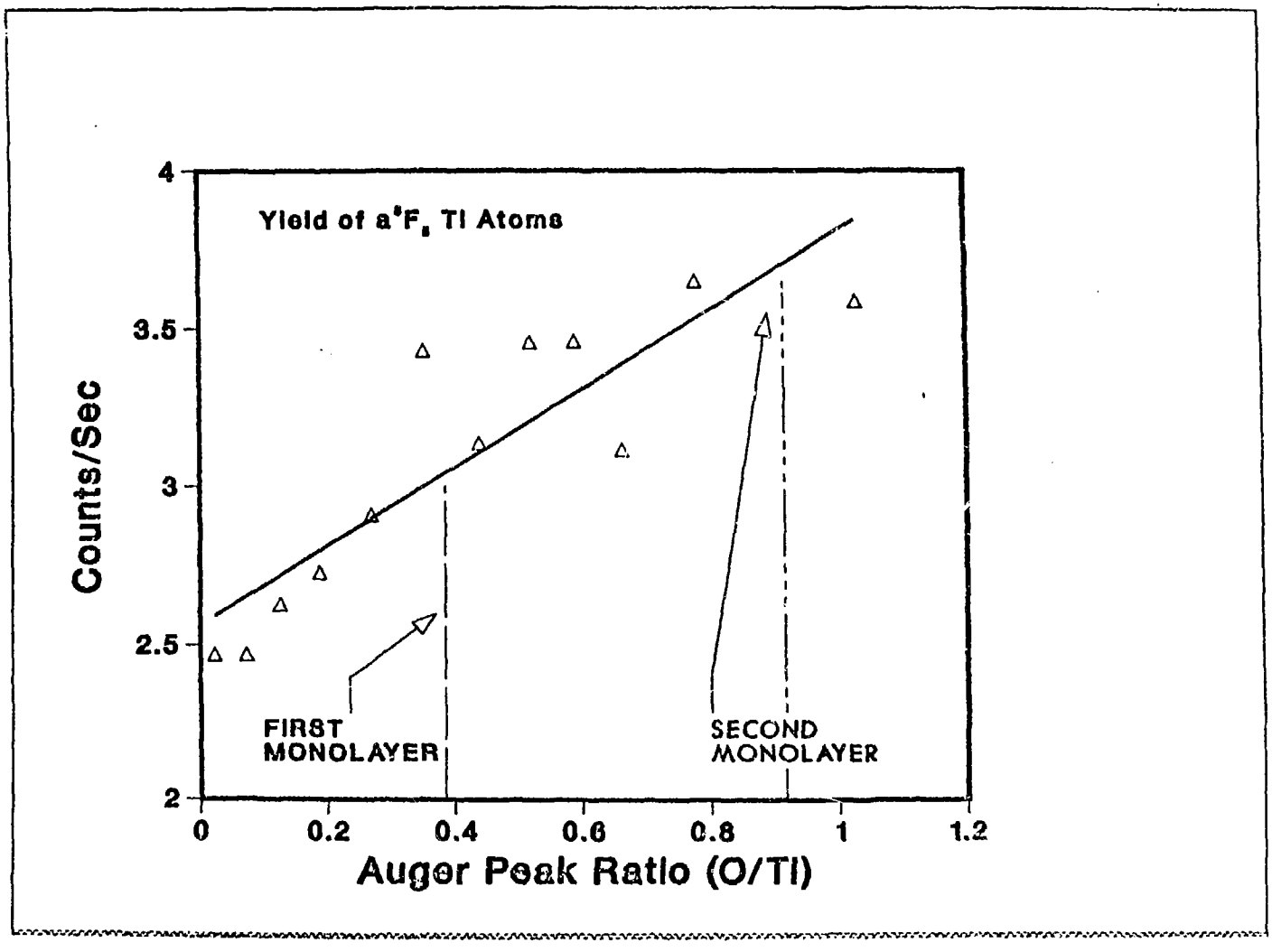
Yield of a$^5F_1$ Tl Atoms
Counts/Sec
4
3.5
3
2.5
2
0
0.2
0.4
0.6
0.8
1
1.2
Auger Peak Ratio (O/Tl)
FIRST MONOLAYER
SECOND MONOLAYER

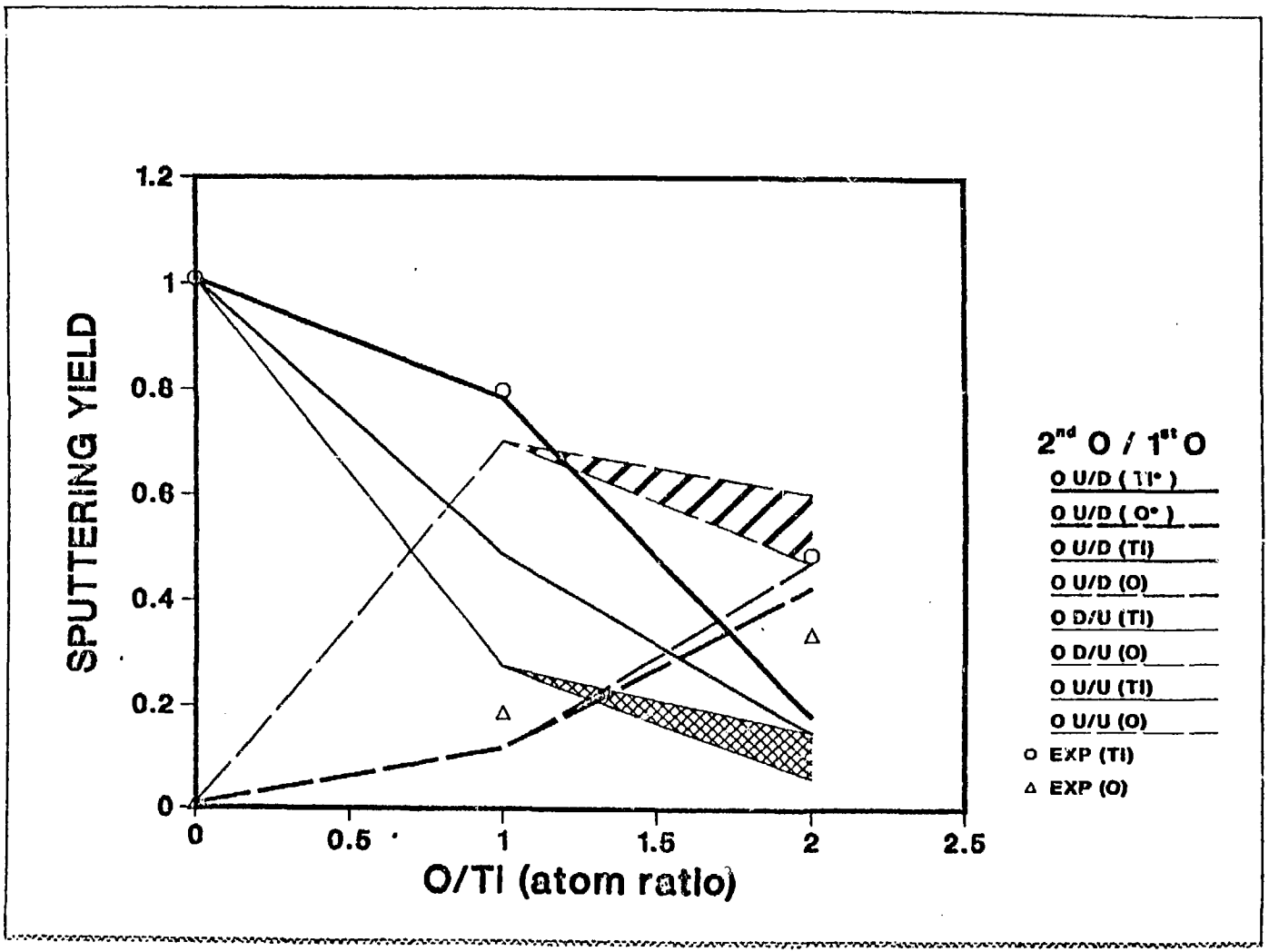
SPUTTERING YIELD
1.2
1
0.8
0.6
0.4
0.2
0
0
0.5
1
1.5
2
2.5
O/Tl (atom ratio)
2nd O / 1st O
O U/D (Tl*)
O U/D (O*)
O U/D (Tl)
O U/D (O)
O D/U (Tl)
O D/U (O)
O U/U (Tl)
O U/U (O)
EXP (Tl)
EXP (O)

DISCLAIMER